Dalton Transactions

PAPER

View Article Online
View Journal | View Issue

Cite this: *Dalton Trans.*, 2017, **46**, 16077

Phosphorescent heterobimetallic complexes involving platinum(IV) and rhenium(VII) centers connected by an unsupported μ-oxido bridge†

Hajar Molaee,[a,b] S. Masoud Nabavizadeh, *[a] Mahboubeh Jamshidi,[a] Max Vilsmeier,[c] Arno Pfitzner[c] and Mozhgan Samandar Sangari[a]

Heterobimetallic compounds [(C^N)LMe$_2$Pt(μ-O)ReO$_3$] (C^N = ppy, L = PPh$_3$, **2a**; C^N = ppy, L = PMePh$_2$, **2b**; C^N = bhq, L = PPh$_3$, **2c**; C^N = bhq, L = PMePh$_2$, **2d**) containing a discrete unsupported Pt(IV)–O–Re(VII) bridge have been synthesized through a targeted synthesis route. The compounds have been prepared by a single-pot synthesis in which the Pt(IV) precursor [PtMe$_2$I(C^N)L] complexes are allowed to react easily with AgReO$_4$ in which the iodide ligand of the starting Pt(IV) complex is replaced by an ReO$_4^-$ anion. In these Pt–O–Re complexes, the Pt(IV) centers have an octahedral geometry, completed by a cyclometalated bidentate ligand (C^N), two methyl groups and a phosphine ligand, while the Re(VII) centers have a tetrahedral geometry. Elemental analysis, single crystal X-ray diffraction analysis and multinuclear NMR spectroscopy are used to establish their identities. The new complexes exhibit phosphorescence emission in the solid and solution states at 298 and 77 K, which is an uncommon property of platinum complexes with an oxidation state of +4. According to DFT calculations, we found that this emission behavior in the new complexes originates from ligand centered ^{3}LC (C^N) character with a slight amount of metal to ligand charge transfer (^{3}MLCT). The solid-state emission data of the corresponding cycloplatinated(IV) precursor complexes [PtMe$_2$I(C^N)L], **1a–1d**, pointed out that the replacement of I$^-$ by an ReO$_4^-$ anion helps enhancing the emission efficiency besides shifting the emission wavelengths.

Received 23rd August 2017,
Accepted 26th October 2017

DOI: 10.1039/c7dt03126b

rsc.li/dalton

1. Introduction

The chemistry of small molecules and clusters involving heterobimetallic M–O–M′ frameworks is of special interest in recent years due to their different applications in many commercially important systems.[1–6] Heterobimetallic systems including μ-oxo-bridge complexes have often been used by nature to catalyze significant reactions in biology.[7,8] These complexes are also used as soluble molecular analogues for molecular catalysts immobilized on metal oxide supports.[9,10] The interesting properties of heterobimetallic complexes arise from the possible "synergistic" effect of two different metal ions held together in close proximity. The metal centers can be placed in close proximity by using an oxygen bridge, which allows a more distinct chemical communication between the two metal centers. These observations encourage chemists to synthesize heterobimetallic compounds involving two different metal centers connected by an unsupported oxido bridge, the idea being that such a system will be more efficient than the one involving the individual metal centers for various fundamental reactions.[11–14] The synthesis of advanced multifunctional materials can also be envisaged through the combination of metal centers with catalytic and optical properties.

One of the best and more successful methods for the preparation of μ-oxo-bridge mixed-metal complexes is using the metal oxyanions such as CrO$_4^{2-}$, MoO$_4^{2-}$ and ReO$_4^-$ as ligands for metal cations. A search in the literature showed that there are many complexes containing ReO$_4^-$ coordinated to transition metal centers.[5,12,15] The use of platinum remains surprisingly underexplored. Very recently, we reported an oxo-bridge Pt–O–Re system obtained from the oxidative addition of methyltrioxorhenium to the [PtMe$_2$bpy] (bpy = 2,2′-bipyridine) complex.[16]

Lots of photophysical studies have been performed on the complexes of d^6, such as Ru(II),[17] Os(II)[18] and Ir(III)[19] and d^8

[a]Department of Chemistry, College of Sciences, Shiraz University, Shiraz, 71467-13565, Iran. E-mail: nabavizadeh@shirazu.ac.ir
[b]Department of Chemistry, University of Isfahan, Isfahan 81746-73441, Iran
[c]Institut für Anorganische Chemie, Universität Regensburg, 93040 Regensburg, Germany

†Electronic supplementary information (ESI) available. CCDC 1545899. For ESI and crystallographic data in CIF or other electronic format see DOI: 10.1039/c7dt03126b

such as Pt(II)[20–22] ions, but the excited-state properties of Pt(IV) complexes have been scarcely studied.[23–28] The first Pt(IV) organometallic emitters were published in 1986 by Balzani *et al.* These neutral bis-cyclometalated platinum complexes have the type $[Pt(C^N)_2(R)Cl]$ [C^N = cyclometalated 2-phenylpyridinate (ppy) or 2-thienylpyridinate (thpy); R = CH_2Cl, $CHCl_2$], which emit from the lowest triplet ligand centered excited state.[23] Bis-cyclometalated platinum(IV) complexes of the type $[Pt(C^N)_2(N^N)](PF_6)_2$ (N^N = aromatic diimine),[24] having at least two cyclometalated rings in their structures and mono cyclometalated Pt(IV) emitters in $[Pt(C^N)L_2MeI]$ [C^N = cyclometalated 3-perylenylmethylen-4′-ethylaniline][25] are the examples of emissive Pt(IV) complexes.

Herein, we report the synthesis of four luminescent heterobimetallic compounds with the general formula $[(C^N)LMe_2Pt(\mu\text{-}O)ReO_3]$ (C^N = ppy, L = PPh_3, **2a**; C^N = ppy, L = $PMePh_2$, **2b**; C^N = bhq (benzo[h]quinolate), L = PPh_3, **2c**; C^N = bhq, L = $PMePh_2$, **2d**), with a hitherto unknown unsymmetrical combination involving a cycloplatinated(IV) and a rhenium(VII) center, connected together by a sole μ-oxido bridge. Thus, the treatment of cycloplatinated(IV) complexes with $AgReO_4$ led to the isolation of compounds involving Pt(IV)–O–Re(VII) units, which are the first example of an organo cyclometalated platinum(IV) complex coordinated to perrhenate. One of these compounds, **2d**, has been structurally characterized by single crystal X-ray diffraction analysis. Their photophysical behavior has also been explored in detail. As far as we know, the Pt(IV) complexes discussed in this paper constitute the first examples of luminescent heterobimetallic Pt(IV) complexes.

2. Experimental section

2.1. Materials and methods

The ^1H, ^{13}C and ^{31}P NMR spectra were recorded on a Bruker Avance DRX 400 MHz spectrometer. The chemical shifts and coupling constants are in ppm and Hz, respectively. $AgReO_4$ was commercially available and the precursor compounds $[PtMe_2I(C^N)L]$, **1a–d**, (C^N = ppy or bhq and L = PPh_3 or $PMePh_2$) were prepared according to reported procedures.[29] Microanalyses for CHN were performed using a Thermo Finnigan Flash EA-1112 CHNSO rapid elemental analyzer. The UV-vis absorption spectra were recorded on a PerkinElmer Lambda 25 spectrophotometer using a cuvette with a path length of 1 cm and/or 1 mm. Excitation and emission spectra were obtained on a PerkinElmer LS45 fluorescence spectrometer with the lifetimes measured in phosphorimeter mode. Absolute measurements of the photoluminescence quantum yield at ambient temperature were performed using a C9920-02 (Hamamatsu Photonics) system equipped with a Spectralon® integrating sphere.

2.2. Synthesis of complexes

$[(ppy)(PPh_3)Me_2Pt(\mu\text{-}O)ReO_3]$, 2a. $AgReO_4$ (116 mg, 0.32 mmol) was added to a solution of $[PtMe_2I(ppy)(PPh_3)]$ (0.050 g, 0.065 mmol) in $CHCl_3$ (20 mL). The reaction mixture was stirred for 1 h at room temperature. Then the reaction mixture was filtered and the solvent was evaporated to give a precipitate. Furthermore, it was washed with pentane (10 mL) and dried under vacuum. The white powder product was obtained. Yield 75%. M.p. 151 °C (decomp.). Anal. calc. for $C_{31}H_{29}NO_4PPtRe$, C, 41.57; H, 3.28; N, 1.57%; found, C, 41.32; H, 3.24; N, 2.02%. ^1H NMR in $CDCl_3$: δ 0.90 (d, $^2J_{PtH}$ = 55.6 Hz, $^3J_{PH}$ = 8.1 Hz, 3H, Me *trans* to P), 1.38 (d, $^2J_{PtH}$ = 65.8 Hz, $^3J_{PH}$ = 8.2 Hz, 3H, Me *trans* to N), 7.01 ($^3J_{PtH}$ = 24.0 Hz, $^3J_{HH}$ = 8.2 Hz, 1H, the CH group adjacent to the ligating C atom of ppy), 8.42 ($^3J_{PtH}$ = 8.6 Hz, $^3J_{HH}$ = 4.8 Hz, 1H, the CH group adjacent to the ligating N atom of ppy). ^{13}C NMR in $CDCl_3$: 0.07 (d, $^1J_{PtC}$ = 659.2, $^2J_{PC}$ = 3.8 Hz, the 1C atom of the Me ligand *trans* to the ligating N atom), 14.65 (d, $^1J_{PtC}$ = 512.5 Hz, $^2J_{PC}$ = 102.2 Hz, 1C atoms of the Me ligand *trans* to the ligating P atom), 119.64–159.48 (29C aromatics).^{31}P NMR in $CDCl_3$: 7.9 ppm (s, $^1J_{PtP}$ = 1004 Hz).

$[(bhq)(PMePh_2)Me_2Pt(\mu\text{-}O)ReO_3]$, 2d. $AgReO_4$ (122 mg, 0.34 mmol) was added to a solution of $[PtMe_2I(bhq)(PPh_3)]$ (0.050 g, 0.068 mmol) in $CHCl_3$ (20 mL). The reaction mixture was stirred for 2 h at room temperature. Then the reaction mixture was filtered and the solvent was evaporated to give a bright yellowish precipitate. Furthermore, it was washed with *n*-hexane (10 mL) and dried under vacuum. Yield 90%. M.p. 144 °C (decomp.). Anal. calc. for $C_{28}H_{27}NO_4PPtRe$, C, 39.39; H, 3.19; N, 1.64%; found, C, 38.86; H, 3.32; N, 1.60%. ^1H NMR in $CDCl_3$: δ 0.72 (d, $^2J_{PtH}$ = 53.7 Hz, $^3J_{PH}$ = 7.6 Hz, 3H, Me *trans* to P), 1.31 (d, $^2J_{PtH}$ = 66.1 Hz, $^3J_{PH}$ = 8.3, 3H, the Me ligand *trans* to N), 1.57 (d, $^3J_{PtH}$ = 14.2, $^2J_{PH}$ = 9.2 Hz, 3H, Me of the $PMePh_2$ ligand), 7.1 (d, $^3J_{PtH}$ = 18.8 Hz, $^3J_{HH}$ = 6.5, 1H, CH group adjacent to the ligating C atom of bhq), 7.1 (d, $^3J_{PtH}$ = 8.9 Hz, $^3J_{HH}$ = 4.8 Hz, 1H, CH group adjacent to the ligating N atom of bhq). ^{13}C NMR in $CDCl_3$: 0.97 (d, $^1J_{PtC}$ = 654.8 Hz, $^2J_{PC}$ = 4.0 Hz, the 1C atom of the Me ligand *trans* to the ligating N atom), 9.00 (d, $^2J_{PtC}$ = 18.4 Hz, $^1J_{PC}$ = 28.6 Hz, 1C atoms of Me of $PMePh_2$ ligands *trans* to the ligating P atom), 13.73 (d, $^1J_{PtC}$ = 504.4 Hz, $^2J_{PC}$ = 107.5 Hz, the 1C atom of the Me ligand *trans* to the ligating P atom), 119.67 (s, $^2J_{PtC}$ = 15.4 Hz), 159.19 ($^2J_{PtC}$ = 61.4 Hz). ^{31}P NMR in $CDCl_3$: −6.93 (s, $^1J_{PtP}$ = 1079 Hz, 1P).

Complexes **2b** and **2c** were prepared in an analogous manner to complexes **2a** and **2d**, respectively, using the appropriate Pt complex.

$[(ppy)(PMePh_2)Me_2Pt(\mu\text{-}O)ReO_3]$, 2b. Yield: 65%, M.p. 123 °C. Anal. calc. for $C_{26}H_{27}NO_4PPtRe$, C, 37.63; H, 3.28; N, 1.69%; found, C, 37.12; H, 3.42; N, 1.64%. ^1H NMR in $CDCl_3$: δ 0.81 (d, $^2J_{PtH}$ = 54.6 Hz, $^3J_{PH}$ = 7.51 Hz, 3H, the Me ligand *trans* to the ligating P atom), 1.31 (d, $^2J_{PtH}$ = 65.5 Hz, $^3J_{PH}$ = 8.9 Hz, 3H, the Me ligand *trans* to the ligating N atom), 1.60 (d, $^2J_{PH}$ = 8.7 Hz, $^3J_{PtH}$ = 14.3 Hz, 3H, Me of $PMePh_2$), 7.11 (d, $^3J_{PtH}$ = 23.7 Hz, $^3J_{HH}$ = 2.5 Hz, the CH group adjacent to the ligating C atom, 1H), 8.30 (d, $^3J_{PtH}$ = 8.8 Hz, $^3J_{HH}$ = 4.9 Hz, the CH group adjacent to the ligating N atom, 1H). ^{13}C NMR in $CDCl_3$: −1.0 (d, $^1J_{PtC}$ = 654.5 Hz, $^2J_{PC}$ = 3.9 Hz, the 1C atom of the Me ligand *trans* to the ligating N atom), 8.32 (d, $^2J_{PtC}$ = 18.24 Hz, $^1J_{PC}$ = 28.9 Hz, 1C atoms of Me of $PMePh_2$ ligands), 13.7 (d, $^1J_{PtC}$ = 502.59 Hz, $^2J_{PC}$ = 108.61 Hz, the 1C atom of the

Me ligand *trans* to the ligating P atom), 120–160 (23 C_{Ar}). ^{31}P NMR in $CDCl_3$: −7.0 (s, $^1J_{PtP}$ = 1077 Hz, 1P).

[(bhq)(PPh$_3$)Me$_2$Pt(μ-O)ReO$_3$], 2c. Yield: 76%, M.p. = 175 °C (decomp.). Anal. calc. for $C_{33}H_{29}NO_4PPtRe$, C, 43.28; H, 3.19; N, 1.53%; found, C, 42.84; H, 2.93; N, 1.44%. ^{1}H NMR in $CDCl_3$: δ 0.94 (d, $^2J_{PtH}$ = 55.1 Hz, $^3J_{PH}$ = 7.5 Hz, 3H, the Me ligand *trans* to the ligating P atom), 1.60 (d, $^2J_{PtH}$ = 67.6 Hz, $^3J_{PtH}$ = 7.5 Hz, 3H, the Me ligand *trans* to the ligating N atom), 7.12 (d, $^3J_{PtH}$ = 15.5 Hz, $^3J_{HH}$ = 1.7, the CH group adjacent to the ligating C atom), 7.71 (d, $^3J_{PtH}$ = 8.7 Hz, $^3J_{HH}$ = 4.8 Hz, the CH group adjacent to the ligating N atom). ^{13}C NMR in $CDCl_3$: −0.27 (d, $^1J_{PtC}$ = 653.0 Hz, $^2J_{PC}$ = 3.5 Hz, the 1C atom of the Me ligand *trans* to the ligating N atom), 14.3 (d, $^1J_{PtC}$ = 507.7 Hz, $^2J_{PC}$ = 102.2 Hz, 1C atoms of the Me ligand *trans* to the ligating P atom), 122–148 (31 C_{Ar}). ^{31}P NMR in $CDCl_3$: 8.0 (s, $^1J_{PtP}$ = 1022 Hz, 1P).

2.3. Computational details

Gaussian 03[30] was used to fully optimize all the structures at the B3LYP level of density functional theory. The solvation energies were calculated by using the CPCM model in dichloromethane. The effective core potential of Hay and Wadt with a double-ξ valence basis set (LANL2DZ) was chosen to describe Pt, I and Re.[31,32] The 6-31G(d) basis set was used for other atoms.

2.4. Crystallography

Clear yellowish to colorless block-shaped crystals of the complex [(bhq)(PMePh$_2$)Me$_2$Pt(μ-O)ReO$_3$], **2d**, suitable for X-ray crystallography, were grown from a concentrated acetone solution by the slow diffusion of *n*-hexane. The X-ray data of **2d** were collected at T = 123.0(1) K. The data were obtained using the ω scans of 1.0° per frame for 2.5 s using CuK_α radiation. The total number of runs and images was based on the strategy calculation from the program CrysAlisPro.[28] The maximum resolution achieved was Θ = 67.080°. Cell parameters were retrieved using the CrysAlisPro software and refined using CrysAlisPro on 38 635 reflections. Data reduction was performed using the CrysAlisPro software that corrects for Lorentz and polarization effects. The absorption coefficient μ of this material is 19.413 mm^{-1} at this wavelength (λ = 1.54184 Å) and the minimum and maximum transmissions are 0.284 and 0.470. The structure was solved in the space group $P2_1/c$ by intrinsic phasing using the ShelXT[33] structure solution program and refined by least squares using version 2014/7 of ShelXL. All non-hydrogen atoms were refined anisotropically. Hydrogen atom positions were calculated geometrically and refined using the riding model. Crystal data, together with other relevant information on structure determination, are listed in Table 1. CCDC 1545899† contains the supplementary crystallographic data.

Table 1 Crystal data and structure refinement of complex **2d**

Formula	$C_{28}H_{27}NO_4PPtRe$
$D_{calc.}$/g cm^{-3}	2.143
μ/mm^{-1}	19.413
Formula weight/g mol^{-1}	853.76
Color	Clear yellowish to colorless
Shape	Block
Size/mm^3	0.09 × 0.08 × 0.07
T/K	123.0(1)
Crystal system	Monoclinic
Space group	$P2_1/c$
a/Å	18.6078(2)
b/Å	18.5904(2)
c/Å	15.4791(2)
β/°	98.806(1)
V/Å^3	5291.5(1)
Z	8
Wavelength/Å	1.54184
Radiation type	CuK_α
Θ_{min}/°	3.381
Θ_{max}/°	67.080
Measured refl.	59 733
Independent refl.	9445
Reflections with $I > 2\sigma(I)$	9004
R_{int}, R_σ	0.0168, 0.0306
Parameters	655
Restraints	0
Largest peak/e Å^{-3}	0.483
Deepest hole/e Å^{-3}	−0.782
GooF	1.079
wR_2 (all data)	0.0404
wR_2	0.0397
R_1 (all data)	0.0192
R_1	0.0175

3. Results and discussion

3.1. Characterization of the complexes

The compounds reported in this work (**2a–d**) were synthesized as outlined in Scheme 1.

As described in our previous paper,[29] the precursors cycloplatinated(IV) complexes [PtMe$_2$I(C^N)L], **1a–d**, (C^N = ppy or bhq and L = PPh$_3$ or PMePh$_2$) show high stability towards air and moisture in the solid state and in solution for several weeks at ambient temperature. In the presence of $AgReO_4$, the iodide ligand is replaced very easily and cleaned with the added ReO_4^- anion to form the heterobinuclear Pt(IV)–O–Re(VII) products. The perrhenate group is included in the coordination sphere of platinum(IV), *trans* to the C atom of the cyclometalated ligand C^N.

In the ^{1}H NMR spectrum, as shown in Fig. 1, complex **2c** gave two methyl platinum resonances in a 1 : 1 ratio, each of which appeared as a doublet, accompanying with the platinum satellites. The first signal at δ = 0.94 with $^2J_{PtH}$ = 55.0 Hz and $^3J_{PH}$ = 7.2 Hz was assigned to the Me ligand *trans* to the P atom of PPh$_3$, while the second signal at δ = 1.59 that has a higher value of $^2J_{PtH}$ equal to 67.6 Hz (typical of the value for MePt(IV) groups *trans* to nitrogen)[34–36] was attributed to the methyl ligand *trans* to nitrogen. The $^2J_{PtH}$ value for the Me ligand *trans* to the N atom of bhq is larger than that observed for the Me ligand *trans* to the P atom of PPh$_3$ which is due to the lower *trans* influence of a N atom as compared to P. It becomes clear from Fig. 1 that the methyl protons of the starting Pt(IV) complex **1c** are shifted upfield about 0.25 ppm upon coordination to perrhenate to form the heterobinuclear complex **2c** (δ = 1.23 and 1.83 ppm for complex **1c** and 0.94 and 1.59 for complex **2c**, respectively). In the ^{31}P NMR spectrum of complex

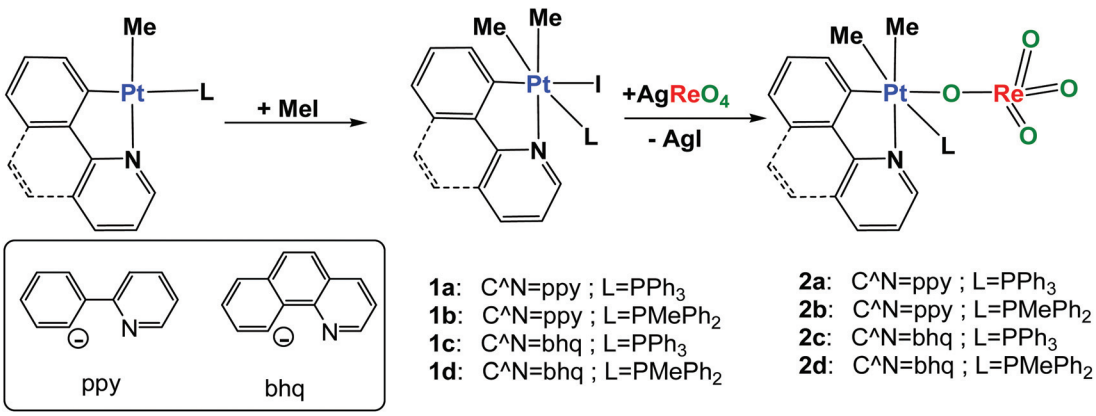

Scheme 1 Schematic presentation for the preparation of complexes **1a–d** and **2a–d**.

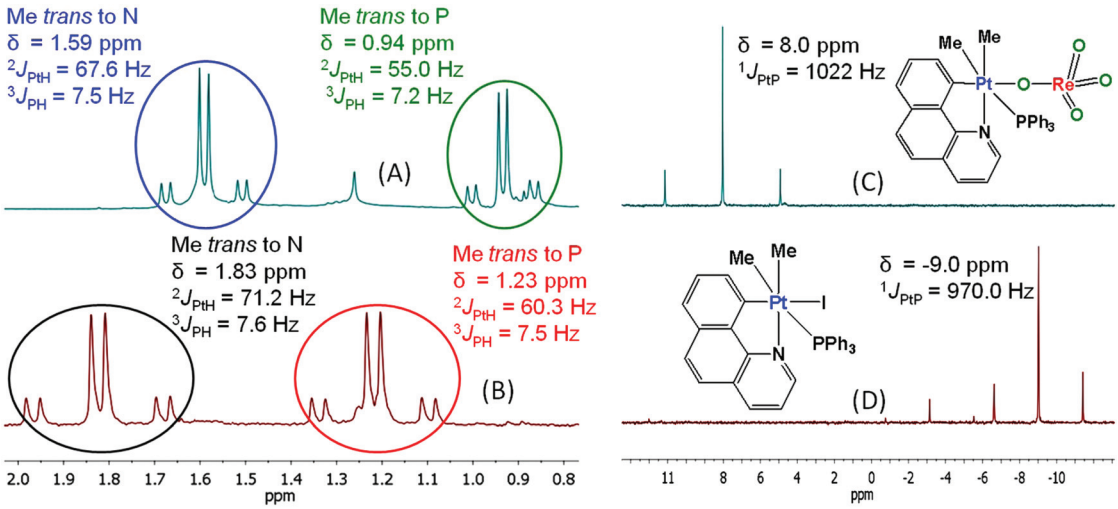

Fig. 1 ^{1}H (Me region, A and B) and ^{31}P (C and D) NMR spectra of complexes **2c** (A and C) and **1c** (B and D).

2c, as expected, a singlet at δ = 8.0 having ^{195}Pt satellites with $^{1}J_{PtP}$ = 1022 Hz was observed, which is shifted as compared to that observed for complex **1c** (δ = −9.0 with $^{1}J_{PtP}$ = 970 Hz).

3.2. Structure description of complex 2d

Clear yellowish to colorless block-shaped crystals of **2d** were obtained from its acetone solution with the slow layer diffusion of *n*-hexane. It crystallizes in the monoclinic crystal system in the space group $P2_1/c$. Two crystallographically different but chemically identical complexes are located in the unit cell. The molecular structures and atom-numbering scheme of **2d**, as well as, selected bond distances and bond angles, are presented in Fig. 2. The crystallographic data and structure analysis of complex **2d** are summarized in Table 1.

As expected, the bhq ligand in complex **2d** binds to the Pt^{IV} metal center *via* one N and one C atom. Two Me ligands take *cis* positions. The perrhenate ion (ReO_4^-) and the bulky phosphine ligand occupy positions in the equatorial plane (*trans* to the ligating C atom of bhq) and the axial positions, respectively. The angles around the Pt center deviate significantly from 90°, *i.e.* the (bhq) bite angles, C25–Pt1–N1 and C54–Pt2–N2 are reduced to 81.66(12)° and 81.86(11)°, respectively, implying that the chelate is probably under strain, whereas the angles formed by the Me ligands *trans* to N with the O atom of ReO_4, *i.e.* O1–Pt1–C2 and O5–Pt2–C30, are increased to 91.86(14)° and 92.90(11)°, respectively.

Different *trans* influences implemented by the $PMePh_2$ ligand and the ligating N atom of bhq are reflected by the bond lengths of the *trans* Pt–Me bonds. For example, due to the larger *trans* influence of a ligating P atom relative to a ligating N atom, the distance of the Pt1–C1 bond *trans* to the $PMePh_2$ ligand (2.081(3) Å) is longer than the distance of the Pt1–C2 bond *trans* to the ligating N atom of bhq (2.058(3) Å). These results are in agreement with the $^{1}J_{PtC}$ values in the ^{13}C NMR spectrum (504.45 and 654.79 Hz for C *trans* to P and C *trans* to N, respectively).

3.3. Structures according to DFT calculations

The structures of complexes **2a–2d** in the gas phase were optimized in S_0 geometry by using DFT calculations (see Fig. S1,

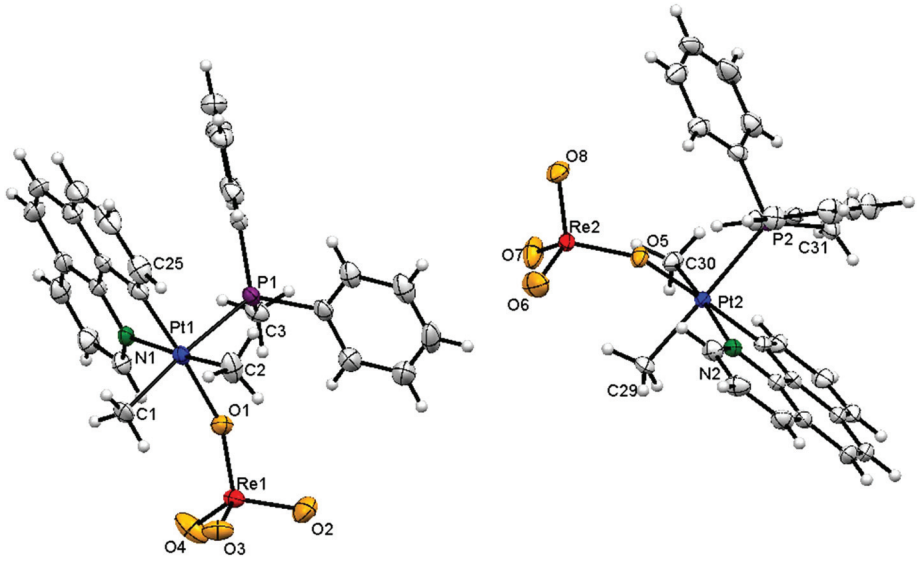

Fig. 2 ORTEP drawing of the two independent molecules of complex **2d** with an atom-numbering scheme. Selected bond lengths (Å) and angles (°): Pt1–P1 2.4020(7), Pt1–O1 2.167(2), Pt1–N1 2.142(2), Pt1–C25 2.000(3), Pt1–C1 2.081(3), Pt1–C2 2.058(3), Pt2–P2 2.3985(7), Pt2–N2 2.144(2), Pt2–O5 2.181(2), Pt2–C54 1.994(3), Pt2–C30 2.063(3), and Pt2–C29 2.093(3); N1–Pt1–C25 81.66(12), N1–Pt1–O1 92.73(10), C25–Pt1–C2 93.76(16), C1–Pt1–O1 89.60(12), O1–Pt1–C2 91.86(14), P1–Pt1–O1 85.59(6), O1–Pt1–C25 174.30(12), N2–Pt2–C54 81.86(11), N2–Pt2–O5 91.05(9), C30–Pt2–C54 94.12(13), C29–Pt2–O5 90.41(11), O5–Pt2–C30 92.90(11), O5–Pt2–C54 172.90(11), and P2–Pt2–O5 89.98(6).

see the ESI† for atomic coordinates and energies of optimized geometries). Selected calculated bond lengths and angles as well as the crystal structure of complex **2d** are given in Table S1.† As is clear from the table, the data of complex **2d** in ground state geometry are in good agreement with the experimental values obtained from single crystal structure determination. Therefore, considering the large molecules under consideration, the B3LYP/LANL2DZ/6-31G(d) method/basis set appears to be a good choice and we used it for the structural characterization of the new heterobinuclear complexes. While the observed Pt–P distance is shorter than that obtained from the calculation, the corresponding Pt–C distances are very close. The differences found in bond distances may indicate the influence of the crystal packing on the experimental bond lengths or may come from the basis sets, which are approximated to a certain extent.[37]

The data reported in Table S1† show again that the *trans* influence of the P atom of PPh_3 is higher than that of the metalated N of bhq. For example for complex **2d**, Pt–C bond lengths *trans* to the P ligating atom of the PPh_3 ligand (Pt1–$C_{(trans\ to\ P)}$ = 2.094 Å) are considerably longer than those of Pt–C bonds *trans* to the N ligating atom of bhq (Pt1–$C_{(trans\ to\ N)}$ = 2.077 Å).

In order to investigate the emission properties, the optimized structures of T_1 geometries were calculated for complexes **2a–2d**. Selected calculated bond lengths and angles of the complexes are given in Table S1.† The deviations of bond lengths compared to the ground state geometry are not so observable, although there are some slight differences in angles. Calculated phosphorescence wavelengths for complexes **1a–1d** and **2a–2d** in the solid phase are reported in Table 3, which are calculated using the energy differences of two states (S_0 and T_1) in their respective minimum geometries.[38] The trends are in good agreement with the experimental data.

3.4. Photophysical properties and TD-DFT calculations

3.4.1. Absorption spectra. The UV–vis absorption spectra of complexes **2a–2d** in dichloromethane at room temperature are shown in Fig. 3 and the resulting photophysical data are reported in Tables 2 and 3.

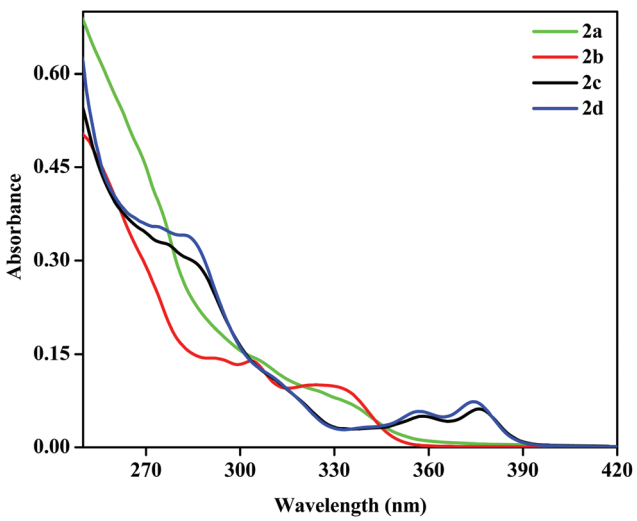

Fig. 3 Absorption spectra of complexes **2a–2d** in dichloromethane solution (3 × 10^{-5} M) at room temperature.

Table 2 Selected vertical singlet excitation of complexes **2a–2d** from TD-DFT calculations in the ground state geometry in CH_2Cl_2 solution, where M = Pt, L = C^N, L′ = phosphine and L″ = ReO_4 (only transitions with a probability higher than 20% are reported)

Complex	Experimental λ [nm]	Calculated λ [nm] (f)	Transitions (probability)	Assignment
2a	329	328 (0.085)	H → L (92%)	LC/L′LCT/MLCT
	307	305 (0.059)	H−1 → L (82%)	LC/L′LCT/MLCT
	270	270 (0.121)	H → L+5 (34%)	LL″CT/L′C/ML′CT
			H−2 → L+1 (26%)	LC/MLCT/L′LCT
2b	324	326 (0.047)	H → L (93%)	LC/L′LCT/MLCT
	304	300 (0.016)	H−1 → L (72%)	LC/L′LCT/MLCT
	294	298 (0.145)	H → L+2 (79%)	LC/L′L″CT/MMCT
		248 (0.09)	H−1 → L+5 (41%)	L′C/LL″CT
2c	376	352 (0.007)	H → L (85%)	LC/L′LCT/MLCT
	358	342 (0.087)	H → L+1 (79%)	LC/L′C
	287	290 (0.055)	H−1 → L+3 (70%)	LC/L′C/MLCT
2d	374	348 (0.075)	H → L (90%)	LC/L′LCT/MLCT
	357	330 (0.032)	H → L+1 (87%)	LC/L′LCT/MLCT
	281	288 (0.191)	H−2 → L (54%)	LC
			H → L+3 (27%)	L′C/LL′CT/ML′CT

Table 3 Photophysical data of complexes **2a–2d** in different media and **1a–1d** in the solid state

Comp.	Media	Temp.	λ_{em} [nm]	τ_{em} (μs)	$\Phi_{PL\ (\%)}$	$\lambda_{Phos.}$ (theo.)	λ_{abs}/nm ($\varepsilon/10^{-4}$ M^{-1} cm^{-1})
1a	Solid	298 K	489, 520_{max}, 562		0.4	427	
1b	Solid	298 K	489, 519_{max}, 560		1.5	422	
1c	Solid	298 K	492, 528_{max}, 580_{max}		0.4	463	
1d	Solid	298 K	479, 513_{max}, 552		0.8	461	
2a	Solid	298 K	480, 510_{max}, 539	36.4	2.5	421	
		77 K	479_{max}, 508, 542				
	CH_2Cl_2	298 K	450, 479_{max}, 510	<1[a]	0.6		329 (0.179), 307 (0.279), 270 (0.899)
		77 K	475, 500_{max}, 533				
	THF	298 K	427_{max}, 467, 516				
		77 K	443_{max}, 475, 504				
2b	Solid	298 K	482, 513_{max}, 543	40.1	3.0	419	
		77 K	478_{max}, 508, 544				
	CH_2Cl_2	298 K	486, 521_{max}, 560	<1[a]	0.7		324 (0.585), 304 (0.808), 294 (0.826)
		77 K	476, 504_{max}, 542				
	THF	298 K	422_{max}, 457, 494				
		77 K	452_{max}, 483, 511				
2c	Solid	298 K	486, 518_{max}, 545	53.9	1.0	459	
		77 K	487, 525_{max}, 580				
	CH_2Cl_2	298 K	484, 520_{max}, 557	4.0	0.8		376 (0.407), 358 (0.33), 287 (1.88)
		77 K	484, 521_{max}, 564				
	THF	298 K	439_{max}, 463, 497				
		77 K	474_{max}, 511, 554				
2d	Solid	298 K	490_{max}, 530, 562	56.0	1.0	457	
		77 K	491_{max}, 529, 570				
	CH_2Cl_2	298 K	483, 516_{max}, 552	20.0	0.6		374 (0.441), 357 (0.348), 281 (2.047)
		77 K	484_{max}, 515, 453				
	THF	298 K	433_{max}, 460, 493				
		77 K	471_{max}, 510, 547				

[a] Lifetime was too short to be measured.

The absorption spectra (Fig. 3) of these compounds display structured bands in the 250–400 nm region, which are similar in shape and energy to those found for the other reported cyclometalated Pt(IV) complexes.[24,27] The relatively intense electronic transitions at higher energies (below 300 nm) are normally assigned to ligand centered metal perturbed (^{1}LC, π → π*) transitions within the C^N (ppy, bhq) and aryl group of the phosphine ligands.[39,40] The absorption bands with a lower intensity observed at λ > 320 nm, presumably having a mixed contribution, as supported by TD-DFT calculations, are attributed to a mixture of spin-allowed ^{1}LC, L′LCT and ^{1}MLCT transitions. Based on the absorption spectra, it seems that the nature of the P ligand (PPh_3 and $PMePh_2$) is less important than the nature of the C^N ligands.

To gain further insight into the absorption transitions of complexes **2a–2d** in dichloromethane, TD-DFT calculations were performed in the optimized ground state geometry (see Fig. 4) and the resulting data and the corresponding wavelengths for the singlet transitions are given in Table 2. The

energies of selected relevant molecular orbitals of complexes **2a–2d** and their compositions in the ground S_0 state are reported in Table S2.† The frontier orbitals and the relative composing energy levels of complexes **2a–2d** are also shown in Fig. S2–S5.† The analysis of the frontier orbitals shows that in complexes **2a** and **2b**, the phosphine ligands have the maximum contribution to the highest occupied MO with some contributions of the Pt center, p_π orbitals of ppy and Me groups. The bhq complexes, **2c** and **2d**, p_π orbitals of bhq have the maximum contribution to the HOMO. The results also show that the contribution of the bhq ligand to the HOMO is larger than that of the ppy ligand in related complexes. As expected, the ReO_4 fragment has no contribution to the HOMO and LUMO, but shows more contributions to higher LUMOs. The LUMOs of complexes **2a–2d** are considerably localized on the C^N ligands.

As shown in Fig. 4 and Table 2, there are some deviations between the experimental and calculated transitions. It should be noted that the energy difference between the electronically singlet excited states and the ground state determined in the ground state geometry (S_0) corresponds to vertical absorption. Complexes **2a** and **2b** show good agreement with experiments but the errors for complexes **2c** and **2d** are 0.22 and 0.25 eV, respectively, which are acceptable for the B3LYP functional.[38,41]

In the spectrum of complex **2a**, the band appearing close to 329 nm has a mixed ^{1}LC, LL′CT and ^{1}MLCT character. In contrast to **2a**, the related band in the spectrum of **2b** (which has a donor group such as Me on the phosphine ligand) is blue-shifted to nearly 324 nm. This blue shift is in agreement with the reduced calculated HOMO–LUMO separation for **2a** (4.447 eV) in comparison with that for **2b** (4.468 eV) (see Table S2†). As seen in the spectrum of **2c**, there are two bands appearing at 376 and 358 nm, having a mixed ^{1}LC, ^{1}L′LCT and ^{1}MLCT character. These bands of complex **2d** appeared at 374 and 357 nm and show again a slight blue shift compared to those for **2c**. These bands in complexes **2c** and **2d** are significantly red-shifted relative to those observed in ppy complexes (329 and 324 nm for complexes **2a** and **2b**, respectively). This is attributed to the extended π-conjugation system in bhq complexes as compared to that for ppy analogues, causing a considerable reduction of the HOMO–LUMO separation for bhq compounds (4.159 and 4.167 eV for **2c** and **2d**, respectively) in comparison with that for ppy analogues (4.447 and 4.468 eV for **2a** and **2b**, respectively).

3.4.2. Emission spectra. The emission properties of the studied complexes were investigated in solid and degassed tetrahydrofuran and dichloromethane solutions at room (298 K) and low temperatures (77 K). The normalized emission spectra of these complexes are shown in Fig. 5, 6 and S6–S8†

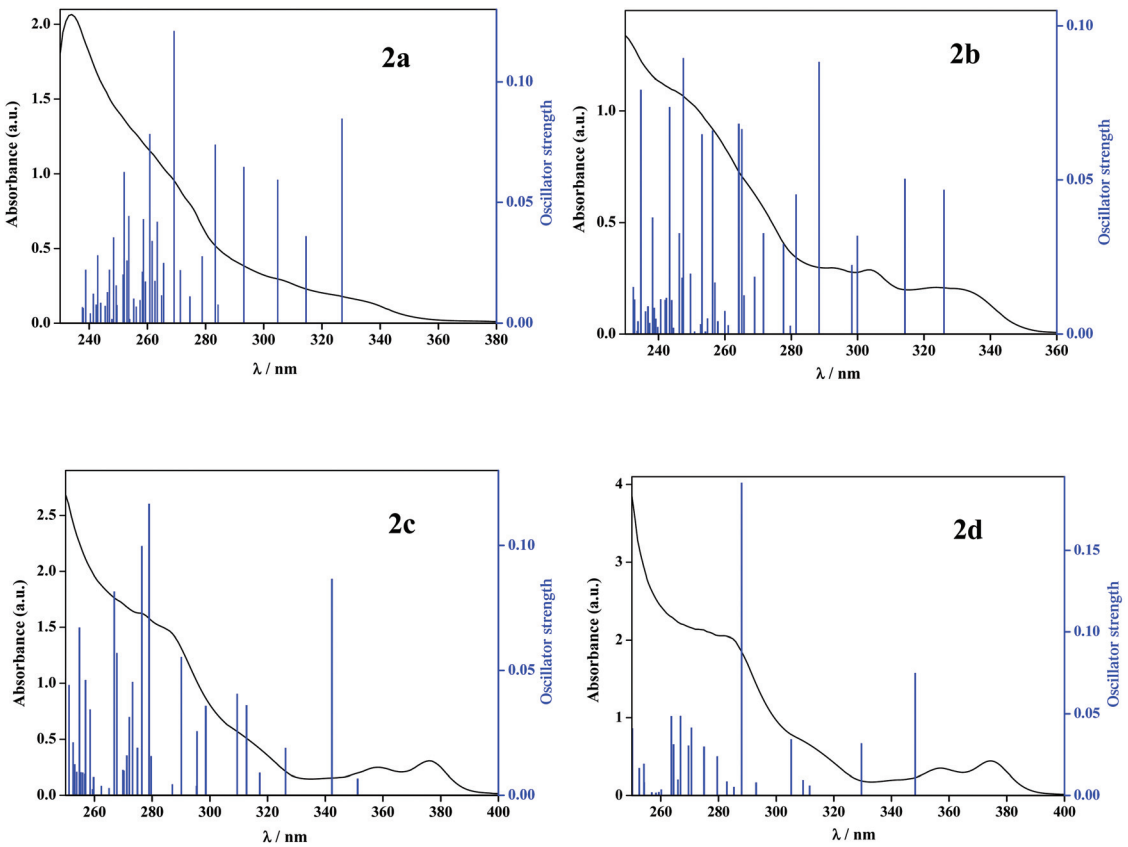

Fig. 4 Overlaid experimental absorbance (spectra) and calculated TD-DFT (bars) of complexes **2a–2d**.

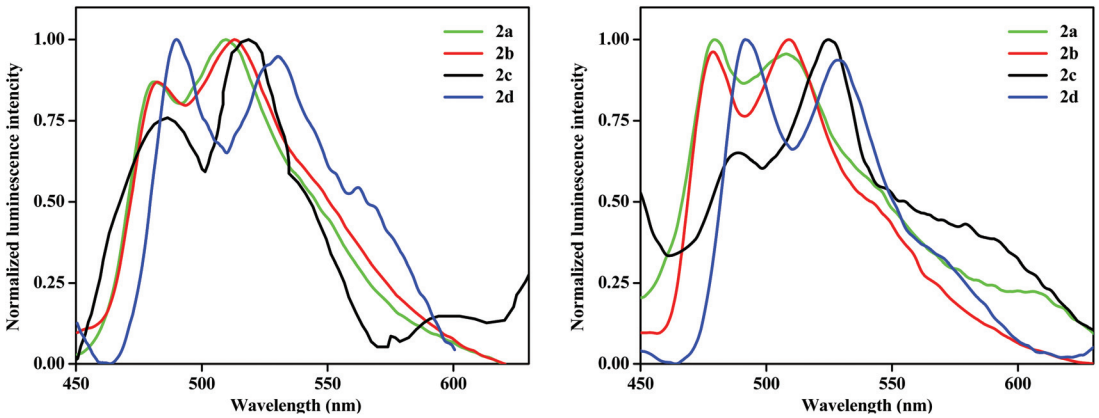

Fig. 5 Normalized emission spectra in the solid state of complexes **2a–2d** (left) at room temperature and (right) at low temperature (77 K).

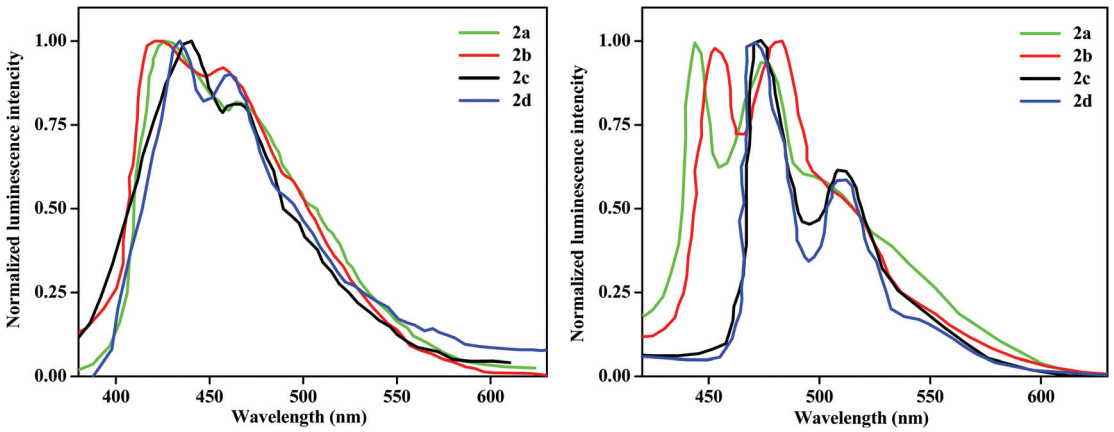

Fig. 6 Normalized emission spectra of complexes **2a–2d** in tetrahydrofuran (left) solution at 298 K and (right) at 77 K.

and the emission data are summarized in Table 3. Moreover, the emission spectra of the precursor complexes (**1a–1d**) were recorded in the solid state.

All complexes are emissive in the solid state. The excited-state lifetimes of the complexes are of the order of micro-seconds, ranging from 36.4 μs to 56.0 μs, showing phosphorescence character and the quantum yields were between 1.0% to 3.0%. The sharply structured emission bands in the solid state at room temperature indicate the presence of a large amount of ligand-centered character in the emissive excited state.[26,27] In this regard, the lower lifetime value of complex **2a** among the heterobimetallic complexes may be due to the less ^{3}LC contribution in its emissive state.[42] Complexes with the bhq ligand (**2c** and **2d**) have larger lifetimes than their corresponding ppy analogues (**2a** and **2b**) due to the expansion of the π-delocalization system.[40] Upon cooling to 77 K in the solid state, the intensities of the emission bands are increased while the band shapes remain similar and show a negligible blue shift to those obtained at 298 K, showing that the complexes are quite rigid even at room temperature.[37]

As shown in Table 3, the emission bands for complexes **2c** and **2d** (having the bhq ligand) appeared at longer wavelengths (*i.e.* red shifted phosphorescence) than those observed for **2a** and **2b**. This is attributed to the expansion of the π-system in the bhq ligand as compared to that in the ppy ligand which leads to the reduction of the π–π* energy gap of the C^N ligands.[39,40,43]

Similar but blue shifted vibrational structured emission bands with the same order in energy shifting as mentioned before can be seen in THF compared to the solid state. This becomes better resolved in the frozen state at 77 K (Fig. 6 and Table 3). These structured bands are indicative of essentially ^{3}LC (C^N) emitting excited states similar to other reported Pt (IV) complexes.[26,27] The emission spectra in THF at 77 K are significantly red shifted as compared to room temperature. For example, compound **2b** has a 30 nm red shift at the peak maxima upon cooling to 77 K which is described as *regidochromism* at 77 K in solution.[44]

The study was carried out using a more polar solvent (CH_2Cl_2) as well to gain insight into the solvent-dependence of the emission spectra (see Fig. S8† and Table 3). The red shifted emission spectra compared to THF, a typical solvatochromic effect, suggest a certain degree of charge transfer for the triplet transition.[43,45] On the other hand, this observation

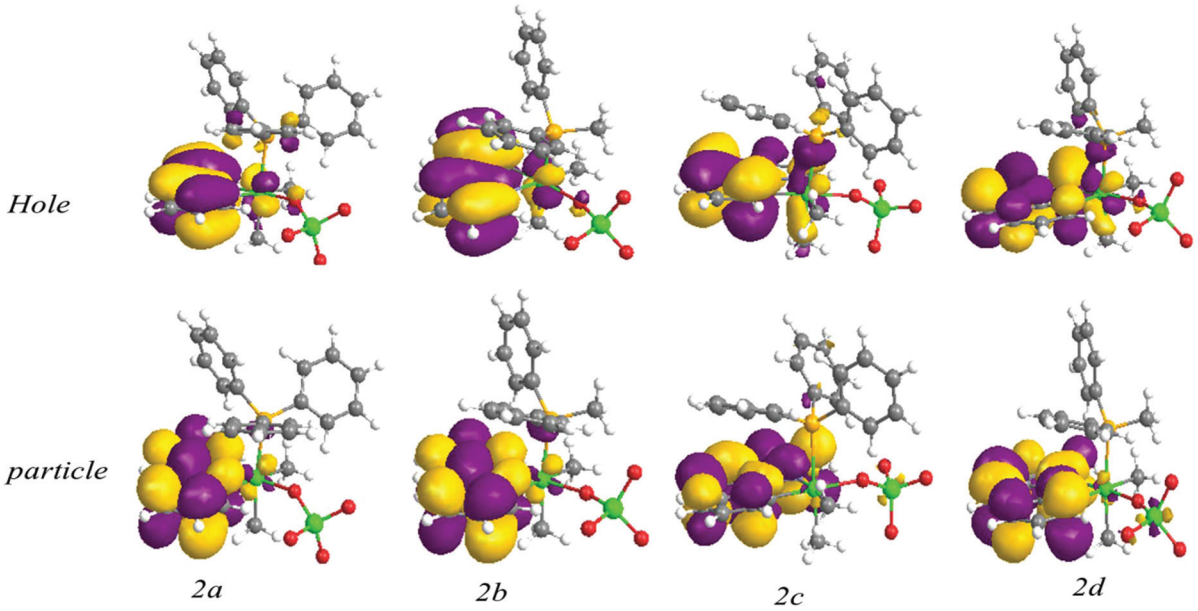

Fig. 7 Natural transition orbitals calculated for the first triplet excited state of complexes **2a–2d**.

proposes that in CH_2Cl_2 the excited state (triplet state) is more stabilized as compared to the ground state, which is due to the higher polarity of the excited state *versus* the ground state and a contribution of ^{3}MLCT character mixed with a ^{3}LC excited state. LMCT character has no role in the emission properties of these compounds, as can be seen in the natural transition orbitals (NTOs) of the first triplet excited state shown in Fig. 7.

As a final point, to illustrate the effect of ReO_4^- on the emission properties of the studied complexes, the emission spectra of the precursor cycloplatinated(IV) complexes (**1a–1d**) were studied in the solid state at 298 K. The normalized emission spectra of these complexes are shown in Fig. 8 and the emission data are summarized in Table 3. As can be seen, all complexes are emissive in the solid state. The emission bands for these complexes have a slight red shift and smaller quantum yields in comparison with those observed for solid **2a–2d** at room temperature (about 0.4% to 1.5%).

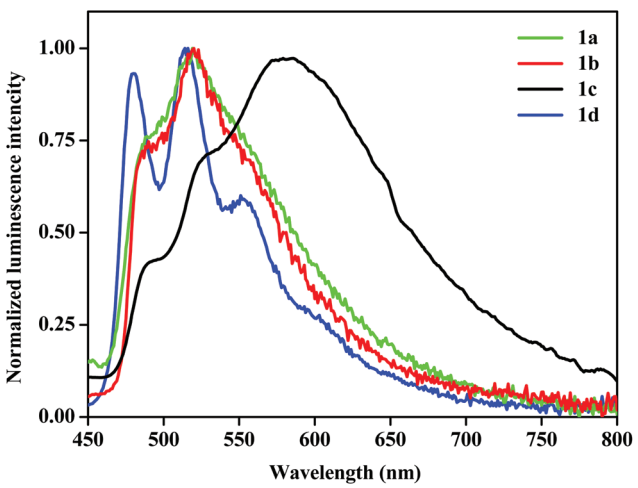

Fig. 8 Normalized emission spectra of complexes **1a–1d** in the solid state at 298 K.

TD-DFT calculations on optimized T_1 geometries of the complexes result the phosphorescence wavelengths as **2a**: 417 nm, **2b**: 417 nm, **2c**: 455 nm, **2d**: 456 nm which are very close to those reported in Table 3. The calculated lowest energy triplet states reproduce the trends observed experimentally for complexes **1** and **2**, so that the emission bands of **1a–1d** appeared at lower wavelengths than those of **2a–2d** (Table 3). NTOs for the lowest-energy triplet excitation in the optimized T_1 geometry (corresponding to phosphorescence) are illustrated in Fig. 7 and 9. Although they show that the C^N and Pt metal center are delocalized over the particle NTOs, remarkably, the character of the hole NTOs of precursor complexes, **1a–1d**, has a different nature compared to that of complexes **2a–2d**. In the former complexes, there is a considerable electron density on the iodide ligand on the hole, without any participation in the excited state. As mentioned above, for complexes **1a–1d**, the emission behavior originates from a mixture of predominant ^{3}LC(C^N) mixed with ^{3}MLCT/^{3}L′LCT character, so the iodide atom has an important role in the emission behavior. However, for compounds **2a–2d** there is no electron density on the ReO_4^- group in the ground state, so this group does not play an important role in the excited state and transition originates from predominant ^{3}LC with minor ^{3}MLCT character. As a result, the replacement of the iodide atom with the ReO_4^- group increases the emission energy and the quantum yield efficiency by changing the character of emission. Although ReO_4^- has no noticeable contribution to the first triplet excited state frontier orbitals, due to the presence of Re as a heavy metal, spin–orbit couplings (SOC) of

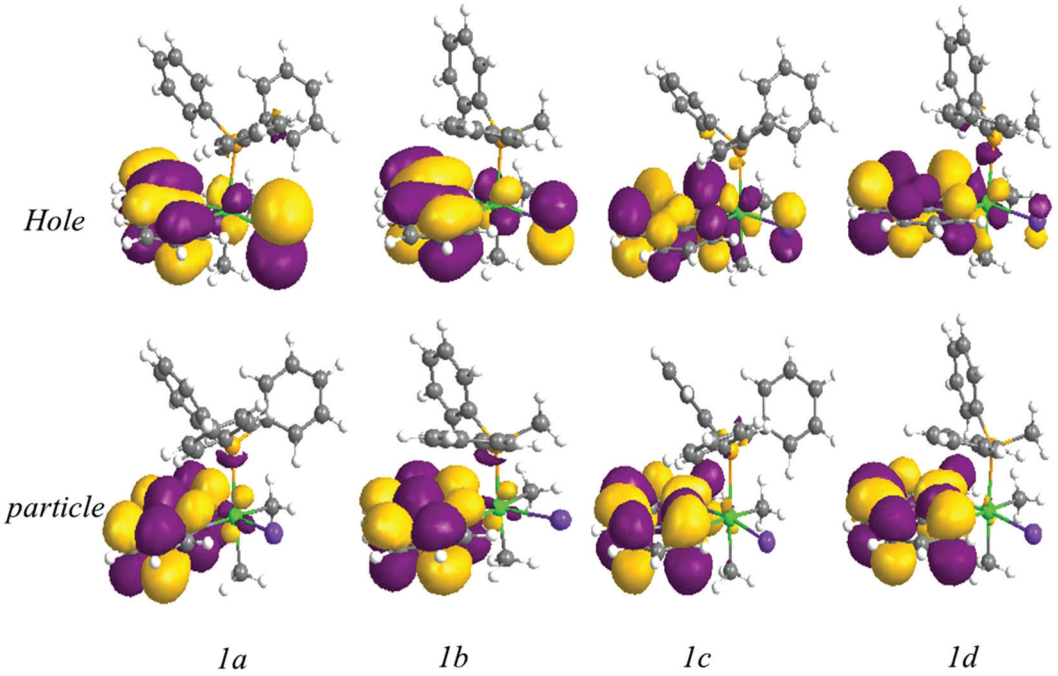

Fig. 9 Natural transition orbitals calculated for the first triplet excited state of **1a–1d**.

such complexes are increased which lead to the enhancement of the intersystem crossing rate constant from the S_1 state to the T_1 state besides more contribution of MLCT character in complexes **2a–2d** compared to **1a–1d**.

4. Conclusions

In this work, a series of heterobimetallic Pt(IV)–O–Re(VII) complexes with the general formula $[(C^N)LMe_2Pt(\mu\text{-}O)ReO_3]$, in which oxygen acts as a mono-bridging atom, were synthesized and characterized. In these complexes, the perrhenate group is included in the coordination site of the Pt(IV) center having an octahedral geometry, completed by a cyclometalated bidentate ligand (C^N), two methyl groups and a phosphine ligand, while the Re(VII) center has a tetrahedral geometry.

Although many photophysical studies have been performed on d^8 Pt(II) complexes and d^6 complexes such as Ru(II) and Ir(III), studies on the photophysical properties of Pt(IV) complexes are scarce and in fact, to the best of our knowledge, the complexes discussed here are the first examples of luminescent heterobimetallic Pt(IV)–Re(VII) complexes. The photophysical properties of these complexes were investigated and the results shown comply well with the DFT and TD-DFT calculations. The following conclusions are drawn by referring to the data obtained:

1- The absorption band of the bhq containing complexes **2c–2d** mildly red shifted as compared to that of the ppy analogue. We consider this behavior to be due to the more extensive π-delocalization in the bhq ligand as compared with that in the ppy ligand. Based on the absorption spectra, it seems that the effect of the nature of the P ligand (PPh_3 and $PMePh_2$) is less important than the effect of the nature of the C^N ligand.

2- In the emission spectra of these Pt(IV)–O–Re(VII) complexes, although the change of the P donor ligand has a mild effect on the wavelength of the related emission band, moving from ppy to bhq (change in the C^N ligand) is moderately effective in this respect. In the emission spectra of the heterobimetallic complexes, the emissive state has predominantly ^{3}LC character with minor ^{3}MLCT character and so the emission band is structured.

3- The solid state emission bands of heterobimetallic compounds show a red shift relative to the corresponding solution state emission bands. For example, the emission band of complex **2d** in THF solution (433 nm) is red shifted to 490 nm in its solid state at 298 K.

4- Upon cooling to 77 K in the solid state, the intensities of the emission bands are increased while the band shapes remain similar to those obtained at 298 K. The heterobimetallic complexes show a blue shift on cooling to 77 K. This observation is attributed to the increased rigidity in the frozen state.

5- It was found that the π–π* energy gap of the cyclometalated ligands plays a significant role in fine-tuning the emission wavelength of the heterobimetallic complexes. This energy gap can be effectively controlled by modifying the C^N backbone and extending the size of the π-conjugation system in the C^N ligand. As found here, expanding the π-conjugated system causes the reduction of the π–π* energy gap leading to a red shift in the emission energy.

6- To illustrate the effect of ReO_4^- on the emission properties of the studied complexes, the emission spectra of the

solid precursors cycloplatinated(IV) complexes (**1a–1d**) were recorded at 298 K. The replacement of iodide with ReO_4^- increased the emission energy and the quantum yield efficiency by omitting the role of the I^- ligand in the excited state.

Conflicts of interest

There are no conflicts to declare.

Acknowledgements

This paper is dedicated to the memory of Prof. Mehdi Rashidi, the father of Organometallic Chemistry in Iran, who passed away on 31 March 2017. He was an exceptionally kind person and an enthusiastic chemist. We deeply miss him. We thank Professors Mahdi M. Abu-Omar and Peter C. Ford for reading and commenting on this manuscript before its submission for publication. We also thank the Iran National Science Foundation (Grant No. 93038832), the Shiraz University and the University of Regensburg for financial support. S. M. N. thanks Shiraz University for providing a sabbatical leave and the University of California, Santa Barbara, for hosting his sabbatical leave during which the writing of this manuscript was completed.

References

1 J. Prakash, G. T. Rohde, K. K. Meier, A. J. Jasniewski, K. M. Van Heuvelen, E. Münck and L. Que Jr., *J. Am. Chem. Soc.*, 2015, **137**, 3478–3481.
2 X. Wu, T. Huang, T. T. Lekich, R. D. Sommer and W. W. Weare, *Inorg. Chem.*, 2015, **54**, 5322–5328.
3 A. Zhou, S. T. Kleespies, K. M. Van Heuvelen and L. Que, *Chem. Commun.*, 2015, **51**, 14326–14329.
4 H. W. Roesky, I. Haiduc and N. S. Hosmane, *Chem. Rev.*, 2003, **103**, 2579–2596.
5 P. B. Chatterjee, S. M. T. Abtab, K. Bhattacharya, A. Endo, E. J. Shotton, S. J. Teat and M. Chaudhury, *Inorg. Chem.*, 2008, **47**, 8830–8838.
6 I. S. Gonçalves, A. D. Lopes, T. R. Amarante, F. A. A. Paz, N. J. Silva, M. Pillinger, S. Gago, F. Palacio, F. E. Kühn and C. C. Romão, *Dalton Trans.*, 2009, 10199–10207.
7 A. Roth, E. T. Spielberg and W. Plass, *Inorg. Chem.*, 2007, **46**, 4362–4364.
8 E. E. Chufán, C. N. Verani, S. C. Puiu, E. Rentschler, U. Schatzschneider, C. Incarvito, A. L. Rheingold and K. D. Karlin, *Inorg. Chem.*, 2007, **46**, 3017–3026.
9 J. T. York, A. Llobet, C. J. Cramer and W. B. Tolman, *J. Am. Chem. Soc.*, 2007, **129**, 7990–7999.
10 S. Kundu, F. F. Pfaff, E. Miceli, I. Zaharieva, C. Herwig, S. Yao, E. R. Farquhar, U. Kuhlmann, E. Bill and P. Hildebrandt, *Angew. Chem., Int. Ed.*, 2013, **125**, 5732–5736.
11 K. Bhattacharya, S. M. T. Abtab, M. C. Majee, A. Endo and M. Chaudhury, *Inorg. Chem.*, 2014, **53**, 8287–8297.
12 J. Małecki, B. Machura, A. Palion, I. Gryca, M. Oboz and T. Groń, *Polyhedron*, 2014, **76**, 10–15.
13 T. Huang, X. Wu, X. Song, H. Xu, T. I. Smirnova, W. W. Weare and R. D. Sommer, *Dalton Trans.*, 2015, **44**, 18937–18944.
14 T. Huang, X. Wu, W. W. Weare and R. D. Sommer, *Eur. J. Inorg. Chem.*, 2014, **2014**, 5662–5674.
15 I. S. Gonçalves, A. D. Lopes, T. R. Amarante, F. A. A. Paz, N. J. Silva, M. Pillinger, S. Gago, F. Palacio, F. E. Kühn and C. C. Romao, *Dalton Trans.*, 2009, 10199–10207.
16 K. R. Pichaandi, L. Kabalan, H. Amini, G. Zhang, H. Zhu, H. I. Kenttämaa, P. E. Fanwick, J. T. Miller, S. Kais, S. M. Nabavizadeh, M. Rashidi and M. M. Abu-Omar, *Inorg. Chem.*, 2017, **56**, 2145–2152.
17 S. Kajouj, L. Marcélis, V. Lemaur, D. Beljonne and C. Moucheron, *Dalton Trans.*, 2017, **46**, 6623–6633.
18 S. Xu, J. E. Smith, S. Gozem, A. I. Krylov and J. M. Weber, *Inorg. Chem.*, 2017, **56**, 7029–7037.
19 Y.-J. Cho, S.-Y. Kim, J.-H. Kim, J. Lee, D. W. Cho, S. Yi, H.-J. Son, W.-S. Han and S. O. Kang, *J. Mater. Chem. C*, 2017, **5**, 1651–1659.
20 M. S. Sangari, M. G. Haghighi, S. M. Nabavizadeh, M. Kubicki and M. Rashidi, *New J. Chem.*, 2017, DOI: 10.1039/c7nj03034g.
21 H. R. Shahsavari, R. B. Aghakhanpour, M. Babaghasabha, M. G. Haghighi, S. M. Nabavizadeh and B. Notash, *New J. Chem.*, 2017, **41**, 3798–3810.
22 S. Y.-L. Leung, S. Evariste, C. Lescop, M. Hissler and V. W.-W. Yam, *Chem. Sci.*, 2017, **8**, 4264–4273.
23 L. Chassot, A. Von Zelewsky, D. Sandrini, M. Maestri and V. Balzani, *J. Am. Chem. Soc.*, 1986, **108**, 6084–6085.
24 D. M. Jenkins and S. Bernhard, *Inorg. Chem.*, 2010, **49**, 11297–11308.
25 F. Juliá, G. Aullón, D. Bautista and P. González-Herrero, *Chem. – Eur. J.*, 2014, **20**, 17346–17359.
26 F. Juliá, D. Bautista and P. González-Herrero, *Chem. Commun.*, 2016, **52**, 1657–1660.
27 F. Juliá, M.-D. García-Legaz, D. Bautista and P. González-Herrero, *Inorg. Chem.*, 2016, **55**, 7647–7660.
28 N. Giménez, R. Lara, M. T. Moreno and E. Lalinde, *Chem. Eur. J.*, 2017, **23**, 5758–5771.
29 S. M. Nabavizadeh, H. Amini, F. Jame, S. Khosraviolya, H. R. Shahsavari, F. N. Hosseini and M. Rashidi, *J. Organomet. Chem.*, 2012, **698**, 53–61.
30 M. J. Frisch, N. Rega, G. A. Petersson, G. W. Trucks, H. Nakatsuji, M. Hada, M. Ehara, K. Toyota, R. Fukuda, J. Hasegawa, M. Ishida, J. C. Burant, T. Nakajima, Y. Honda, O. Kitao, H. B. Schlegel, H. Nakai, M. Klene, X. Li, J. E. Knox, H. P. Hratchian, J. B. Cross, J. M. Millam, V. Bakken, C. Adamo, J. Jaramillo, R. Gomperts, G. E. Scuseria, R. E. Stratmann, O. Yazyev, A. J. Austin, R. Cammi, C. Pomelli, S. S. Iyengar, J. W. Ochterski, P. Y. Ayala, K. Morokuma, G. A. Voth, P. Salvador, M. A. Robb, J. J. Dannenberg, V. G. Zakrzewski,

S. Dapprich, A. D. Daniels, J. Tomasi, M. C. Strain, O. Farkas, D. K. Malick, A. D. Rabuck, K. Raghavachari, J. B. Foresman, J. R. Cheeseman, J. V. Ortiz, Q. Cui, A. G. Baboul, V. Barone, S. Clifford, J. Cioslowski, B. B. Stefanov, G. Liu, A. Liashenko, P. Piskorz, I. Komaromi, J. A. Montgomery Jr., R. L. Martin, D. J. Fox, B. Mennucci, T. Keith, M. A. Al-Laham, C. Y. Peng, A. Nanayakkara, M. Challacombe, P. M. W. Gill, B. Johnson, W. Chen, T. Vreven, M. W. Wong, M. Cossi, C. Gonzalez, J. A. Pople, K. N. Kudin and G. Scalmani, *Gaussian 03, Revision C.02*, 2004.

31 P. J. Hay and W. R. Wadt, *J. Chem. Phys.*, 1985, **82**, 270–283.

32 E. S. Raper, *Coord. Chem. Rev.*, 1985, **61**, 115–184.

33 G. M. Sheldrick, *Acta Crystallogr., Sect. C: Cryst. Struct. Commun.*, 2015, **71**, 3–8.

34 M. Safa and R. J. Puddephatt, *J. Organomet. Chem.*, 2013, **724**, 7–16.

35 M. D. Aseman, M. Rashidi, S. M. Nabavizadeh and R. J. Puddephatt, *Organometallics*, 2013, **32**, 2593–2598.

36 M. Safa, M. C. Jennings and R. J. Puddephatt, *Organometallics*, 2012, **31**, 3539–3550.

37 R. B. Aghakhanpour, S. M. Nabavizadeh and M. Rashidi, *J. Organomet. Chem.*, 2016, **819**, 216–227.

38 C. Adamo and D. Jacquemin, *Chem. Soc. Rev.*, 2013, **42**, 845–856.

39 M. Jamshidi, S. M. Nabavizadeh, H. R. Shahsavari and M. Rashidi, *RSC Adv.*, 2015, **5**, 57581–57591.

40 M. Jamshidi, S. M. Nabavizadeh, H. Sepehrpour, F. N. Hosseini, R. Kia and M. Rashidi, *J. Lumin.*, 2016, **179**, 222–229.

41 J. W. Gauld, *J. Am. Chem. Soc.*, 2005, **127**, 3233.

42 R. B. Aghakhanpour, S. M. Nabavizadeh, M. Rashidi and M. Kubicki, *Dalton Trans.*, 2015, **44**, 15829–15842.

43 A. Bossi, A. F. Rausch, M. J. Leitl, R. Czerwieniec, M. T. Whited, P. I. Djurovich, H. Yersin and M. E. Thompson, *Inorg. Chem.*, 2013, **52**, 12403–12415.

44 J. Brooks, Y. Babayan, S. Lamansky, P. I. Djurovich, I. Tsyba, R. Bau and M. E. Thompson, *Inorg. Chem.*, 2002, **41**, 3055–3066.

45 J. R. Berenguer, Á. Díez, E. Lalinde, M. T. Moreno, S. Ruiz and S. Sánchez, *Organometallics*, 2011, **30**, 5776–5792.